CHAPTER-2

LITERATURE SURVEY

CHAPTER-2

LITERATURE SURVEY

Bubble columns are gas-contacting devices in which gas is dispersed into a pool of liquid by sparging through a distributor. It may be operated in batch mode or continuous mode depending upon whether liquid is flowing or not. Mixing in bubble columns are induced by the motion of bubbles, No external effort is required. Sometimes, liquid is recirculated through an internal or external loop. It is called loop reactor.

Bubbles columns find use in several gas-liquid reactions. If, it is used to carry out a catalytic reaction, the catalyst may be suspended. In such cases, the reactor is called as slurry bubble column. Some of the well reactions carried out in bubble columns are hydrogenation, chlorination, oxygenation, F-T synthesis etc. [Shat et al. (1982)]. These contactors also find use to carry out biochemical operations [Buchholz et al. (1979), Klein et al. (2005)] and wastewater treatment etc.

To understand the performance of bubble columns it is necessary to understand the degree of mixing, which determines the heat and mass transfer coefficients. Since the mixing is induced mixing due to movement of bubbles, the bubble behaviour such as bubble size, is shape and bubble velocity are important parameters.

The observed rate of reaction between the reactants, present in liquid and gas phases depends upon the interfacial area and mass-transfer coefficient. The former is due to the BSD in the column. Mass-transfer coefficient is also expected to depend upon the bubble behaviour.

A discussion on various aspects of bubble behaviour and measurement of gas-liquid interfacial area, based on the available literature is presented in the following section.

2.1 Flow Regime

Though, simple in construction, predicting the performance of a bubble column is a challenging task. No single correlation is available to correlate any aspect of the bubble column, e.g. gas holdup, bubble diameter, interfacial area. It is due to different role of small and large bubbles. Defining different types of flow regimes help in understanding the scope a correlation proposed. Depending on the superficial gas velocity, three different flow regimes have been described in bubble columns. Though, few more less popular flow regimes have been reported in literature [Kumar et al. (1976)].

2.1.1 Homogeneous Flow or Bubbly Flow Regime

At very low superficial gas velocity there are few bubbles only. The bubbles are of almost of uniform size. Kumar et al. (1976) subdivided this into regimes. When the bubbles moved freely as individuals it was named as dispersed flow regime. When the bubbles moved as swarm of bubbles it was named as fluidized regime. The bubble size depends on the specification of the sparger, where the bubbles are found. These bubbles rise vertically undisturbed [Zahradnik and Kastanek (1979)]. Due to the absence of bubble coalescence and bubble breakup the size of the bubbles remain unchanged until they are disengaged from the top. The scope of liquid circulation is more due to small size of bubbles [Kantarci et al. (2005)].

Schumpe and Deckwer (1982) observed that flow regime depends upon the type of sparger also. For sintered plate, homogenous flow regime was observed but for

perforated plate, flow regime is not the same at small values of superficial gas velocity. Thus, role of the sparger in affecting the flow regime or performance of the bubble column was realised.

2.1.2 Heterogeneous Flow Regime

When the superficial gas velocity is increased, the number of bubbles in the column increases. The bubbles are closed enough to interact at initial bubble collisions. The collapsed bubbles move at increased velocity causing a liquid circulation. These liquid circulations have been modelled as liquid circulation cell [Joshi and Sharma (1979)]. Whenever liquid turbulence is high, the large bubbles may break into small bubbles [Hinze (1955)]. Bubbles are of various sizes with wide distribution. The residence time of bubbles is not uniform. Liquid turbulence is generally assumed to be isotropic. The transition from homogeneous to heterogeneous flow regime takes place when superficial gas velocity is in the range of 0.05-0.1 $m.s^{-1}$. For perforated plate, even at small values of superficial gas velocity bubbles of various sizes were observed due to bubble coalescence and this type flow was observed.

Kantarci et al. (2005) observed existence of radial gas hold-up profile. A portion of the gas is transported through the bed in the form of fast moving bubbles. This fraction increases with increasing gas velocity. The mass-transfer coefficient was found to be lower in heterogeneous regime than that in homogeneous flow regime.

2.1.3 Slug Flow Regime

In case of small diameter column (< 0.15m), as the gas velocity increased further, the bubble size increased due to bubble collisions. Therefore, bubble diameter becomes equal to column diameter. The liquid turbulence is not sufficient to break the bubble of this size. Therefore, some of the bubbles form slug and move up in this form.

Schumpe and Deckwer (1982) studied transition of flow regime to slug flow regime for various concentrations of CMC solution in a 0.15 m diameter column. In large column homogeneous flow and churn turbulent flow were observed. Slug flow regime is absent. Some of the flow regimes are shown in Figure 2.1.

Sometimes cellular foam like structure in the bed has been observed. It is not due to any foaming agent but is due to hydrodynamic conditions in the bed. Zahradnik and Kastanek (1997) called this as foam Regime. Kumar et al. (1976) have mentioned two flow regimes namely froth regime and foam regime. The flow regime was based on the values of gas holdup.

Kazakis et al. (2007) defined pseudo-homogeneous flow regime within homogeneous flow regime. The gas holdup increases linearly as superficial gas velocity increases but no uniform radial distribution of bubbles is observed.

Industrial bubble columns operate at gas velocity in the range of 0.01-0.5 $m.s^{-1}$. Since the column diameter is large, slug flow regime is absent in industrial bubble columns. The flow regimes depend on type of gas sparger used, operating gas velocity, fluid properties and column diameter. These parameters also influence bubble size, its distribution, gas holdup, bubble velocity and transfer coefficients.

Study of transition of regime from homogeneous to heterogeneous is important as the hydrodynamic behaviour of the system changes significantly. The gas velocity for transition regime depends on sparger design, physical properties of the system and column dimensions [Thorat and Joshi (2004)], though exact correlation is not available.

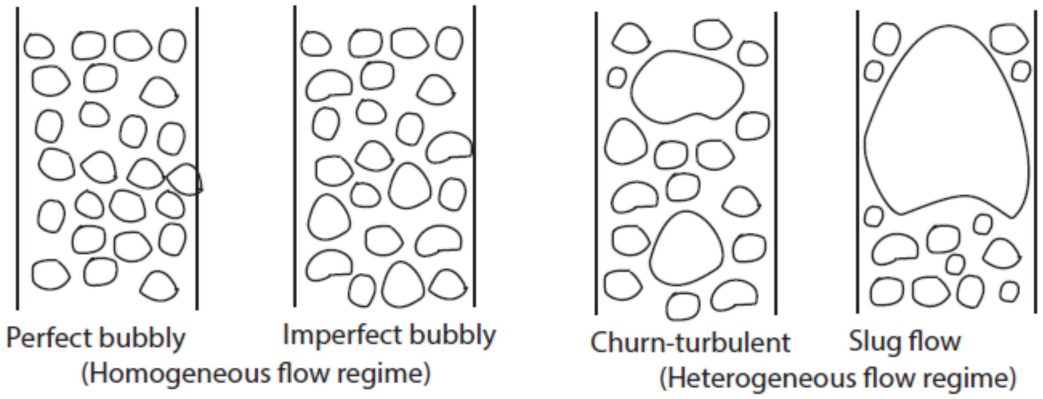

Figure 2.1 Flow regimes in bubble columns (adopted from Reilly et al. (1986))

2.2 Gas Holdup

Gas holdup, ε, in bubble columns have been studied extensively and have been reviewed from time to time. It is defined as ratio of volume fraction of gas phase in the form of gas bubbles to the total volume of gas-liquid dispersion. It is considered to be an important hydrodynamic parameter which affects even transport properties in bubble columns [Verma (1989), Verma and Rai (2003)]. Various correlations for gas holdup proposed in the literature are presented in Table 2.1.

Comparing the correlations of Bach and Pilhofer (1978), Akita and Yoshida (1973), Hikita et al. (1980) and Koide et al. (1984), it is observed that the powers of *Bo*, *Fr*. *Ga* and *Re* are different in each of these correlations because each group of investigators have correlated different functions of *ε*. Akita and Yoshida (1973) and Koide et al. (1984) used. $\varepsilon/(1-\varepsilon)^4$, Bach and Pilhofer (1978) used $\varepsilon/(1-\varepsilon)$ and Hilkita et al. (1980) used ε to correlate their data. Only Hikita et al. (1980) used all four dimensionless numbers. They also used density ratio and viscosity ratio of gas and liquid phases.

Guy et al (1986) studied the effect of number of holes in the sparger, position of holes on perforated plate sparger. The holes were distributed either symmetrically or on one side of the on the perforated plate. While the number of holes affected gas holdup strongly at high superficial gas velocity, the effect of viscosity had significant effect only at low gas velocities. The correlation for gas holdup was in terms of dimensionless numbers though the Ga_o and Fr_o were based on orifice dimensions replacing column diameter. The equivalent diameter, D_E, was same as column diameter, D, in case of symmetrical sparger. When holes were placed on one side of the distributor plate, the value of D_E was taken as ratiof of area of zone on plate having holes to perimeter of the plate.

The most important single parameter affecting gas holdup is superficial gas velocity, which can be seen in several correlations e.g. correlations by Hughmark (1967), Schumpe and Deckwer (1982), Deckwer et al. (1982), Choi et. al. (1996) etc. These correlations did not consider fluid properties. Reilly et al. (1986) tried to study the effect fluid properties and proposed correlations considering data available in literature. It was observed that the previous correlations estimated widely different values of gas holdup even for air-water system. The effect of liquid viscosity on gas holdup has been debated. The correlation of Reilly et al. (1986) shows no effect of viscosity. In the correlation by Godbole et al. (1982) the exponent of the viscosity is -0.058 showing a week dependence of viscosity on gas holdup. Urseanu et. al. (2003) proposed a correlation for gas holdup with exponent of vliquid viscosity as -0.12. Correlation by Anabtawi et. al. (2003) has the exponent eiqal to -0.38 for cylindrical column and -0.22 for two-dimensional column. It shows a much stronger effect of viscosity than that obtained by Godbole et al. (1982). Shumpe and Deckwer (1982) observed no effect of viscosity in case of slug flow regime. However, different

correlations for different columns and homogeneous and slug flow regimes were proposed. The gas holdup increased monotonically with superficial gas velocity.

Surface tension affect gas holdup strongly. The exponent of surface tension in various correlations varied in the range of -0.12 to -0.54[Reilly et al (1986), Pohorecki et. al. (2001), Asgharpour et. al. (2010)]. It is attributed to the fact that low surface tension fluids suppress bubble coalescence. Anastasiou et. al. (2010) proposed different correlations for ionic and non-ionic surfactants.

There is a lack of single correlation for gas holdup. Geometrical parameters such as type of the sparger is one of the major parameters which might be affecting the gas holdup and other properties. Earler correlations considered column diameter, D, as the only geometrical parameter. To include the effect of sparger ratio of hole dia, d_o, to to D was used in the correlation [Mok et. al. (1990), Mouza et. al. (2005)]. Jin et. al. (2013) used free area, number of holes, n_o, d_o and d_o/D. The gas holdup showed strong dependence on free area. Since the correlation used free area as one of the parameters, it can easily be used to correlate the data in bubble columns of square-cross section. Behkish et. al. (2006) took into account sparger geometry, by using n_o, d_o and D.Gas velocity based on nozzle diamter has also been attempted [Guy et. al. (1986)]. Kazakis et. al. (2007) used two dimensionless parameters d_s/D and d_o/D. Anastasiou et. al. (2013) used porous plate of diamter of 0.045 m with pore diameter of 40 μm. The correlation for gas holdup was in terms of Fr, Ar, Eo, d_s/D and d_s/d_o. Sauter-mean bubble diameter, d_{32}, has also been used to include the effect of sparger geometry indirectly [Maceiras et. al. (2010)]. Inclusion of sparger geometry in the correlation seems to be tricky as there are numerous types of spargers used in these studies. Some of these are single nuzzle, multiple nozzle, perforated plate, ring sparger, sintered or porous plate, spider type, cross type etc.

Table 2.1: Correlations for gas holdup in bubble columns (PP=Perforated plate, SN=Single nozzle, SP=Sintered plate), PoP= Porous Plate, RGS= Radial Gas Sparger). The dimensionless numbers used are Eotvos number or Bond's Number, $Eo = Bo = gD^2\rho_l/\sigma_l$; Morton number, $Mo = \mu_l^4 g/\rho_l\sigma^3$; Reynold's number, $\mathrm{Re} = DU_g\rho_l/\mu_l$; Froude number, $Fr = U_g/\sqrt{gD}$; ; Galileo Number, $Ga = gD^3\rho_l^2/\mu_l^2$

Investigator	Correlation	System	Column
Hughmark (1967)	$\varepsilon = \left[1/\left\{2+\left(0.35/U_g\right)\left[\rho_l\left(\sigma_l/0.072\right)\right]^{1/3}\right\}\right]$	Air/water, Versol, Glycerol, Na_2CO_3 soln., $ZnCl_2$ soln.	D=0.0254, 0.0508, 0.1524, 0.3048m
Akita and Yoshida (1973)	$\varepsilon/(1-\varepsilon)^4 = 0.20Bo^{1/8}Ga^{1/12}Fr$	Air, oxygen, helium/water, glycol, glycerol, methanol, 0.15M Sodium sulphite solution	D=0.152, 0.301, 0.6 m SN(d_o=0.005 m)
Kumar et. al. (1976)	$\varepsilon = 0.728U_g^* - 0.485U_g^{*2} + 0.0975U_g^{*3}$ Where $U_g^* = U_g\left[\rho_l^2/\left\{\left(\rho_l-\rho_g\right)\sigma\right\}\right]^{1/4}$	Air, Water, Glycerol (40%),, Kerosene CO_2, Aqueous NaOH (2M)	D=0.05, 0.075, 0.1 m SN (d_o=0.00087, 0.00153, 0.00196, 0.00265, 0.00309 m, n_o=1)
Bach and Pilhofer (1978)	$\varepsilon/\left(1-\varepsilon\right) = 0.115\left(\mathrm{Re}\,Fr'\right)^{0.23}$; $Fr'=Fr^2$	Air, water, butan-1,3-diol, ethylene glycol, tetrabromoethane, n-octanol	D = 0.1 m PP(d_o= 0.0005 m)
Hikita et. al. (1980)	$\varepsilon = 0.672\left(\frac{U_g\mu_l}{\sigma}\right)^{0.578}\left(\frac{\mu_l^4 g}{\rho_l\sigma^3}\right)^{-0.131}\left(\rho_g/\rho_l\right)^{0.062}\left(\mu_g/\mu_l\right)^{0.107}$	Air, H_2, CO_2, CH_4, C_3H_8, N_2, water, sucrose, methaol,	D=0.1 m SN (d_o=0.011 m, n_o=1)

		n-aniline, i-butanol, NaCl, Na_2SO_4, $CaCl_2$, $MgCl_2$, $AlCl_3$, KCl, K_2SO_4, K_3PO4, KNO_3	
Kara et. al. (1982)	$\varepsilon = \mathrm{Re}/(1521.23 + 3.75\,\mathrm{Re})$	Air, water, coal, dried mineral ash	D=0.152 m
Schumpe and Deckwer (1982)	$\varepsilon = 0.0908U_g^{0.85}$ $\varepsilon = 0.0258U_g^{0.876}$ $\varepsilon = 0.0322U_g^{0.674}$ $\varepsilon = 0.404U_g^{0.627}$	Air, CMC (0-2%) Na_2SO_4 (0.8mol/l)	D=0.102, 0.14 m SP (d_o=0.00015, 0.0002 m) PP [(d_o=0.0005 m, n_o=421), (d_o=0.001 m, n_o=73), d_o=0.002 m, d_o=19)]
Deckwer et al. (1982)	$\varepsilon = 0.0265U_g^{0.82}$; for slug flow refime at U_g>0.02 ms^{-1}	Air/Water,CMC solution	D=0.14 m; PP(n_o=73,d_o=0.001m; n_o=19,d_o=0.002m),SP(d_o=0.0002 m); Rubber plate with 1000 pricks
Sada et. al. (1984)	$\varepsilon/(1-\varepsilon)^4 = 0.32Bo^{0.121}Ga^{0.086}(\rho_g/\rho_l)^{0.068}Fr$	N_2, He, CO_2, O_2, glycerol, Na_2SO_4, mixture of LiCl(58 mol%)-KCl(42 mol%) with molten $NaNO_3$	D=0.073 m SN(d_o=0.0015, 0.0027, 0.0057m)
Reilly et. al. (1986)	$\varepsilon = 296U_g^{0.44}\rho_l^{-0.98}\sigma^{-0.16}\rho_g^{0.19} + 0.009$	Air, He, Ar, water, varsol, trichloroethylene, glassbeads	D = 0.3 m PP (d_o=0.0015 m, n_o=293; d_o=0.0134 m, n_o=6), SN(d_o=0.0254 m)
Guy et. al. (1986)	$\varepsilon = 0.386n_oGa_o^{0.025}Fr_o^{0.84}(d_o/D_E)^{2.075}$	Air, water, glycerol, CMC,	D=0.254 m PP [(d_o=0.001 m, n_o=60),

		polyacrylamide Separan	(d_o=0.001 m, n_o=61), (d_o=0.001 m, d_o=33)]
Renjun et. al. (1988)	$\varepsilon = 0.17283 Mo^{-0.1544}\left(P+P_S\right)/P^{1.6105}\left(U_g\mu_l/\sigma\right)^{0.5897}$	Air, water, alcohol, 5% NaCl	D=0.1 m SN(d_o=0.01 m)
Bukur and Patel (1989)	For pure liquids same as Bach and Pilhofer (1978) $\varepsilon = U_g^{K_1}(1+C_N)^{0.167}\Big/\left(K_2+\left\{K_3/U_g^{K_4}\right\}\left\{\rho_l\sigma/0.072\right\}^{K_5}\right)$; ($C_N$ is carbon number, for butanol solution) $\varepsilon/(1-\varepsilon)^4 = 0.032 Bo^{-0.056} Ga^{0.31} Fr^{1.2} We^{0.25}$; (for PP and SN distributors, solutions) $\varepsilon = 1.42 U_g \mu_l^{-0.27}$; (for SP distributor, solutions)	N_2, water, n-butanol, CMC	[D=0.05 m; SN(d_o=0.001, 0.00185m), SP(d_o=40μm)], D=0.23 m; PP(n_o=19, d_o=0.001,0.00185m)
Kawase and Moo-Young (1989)	$\varepsilon = 1.07(1-a)^{1/3} Fr^{1/3}; a = \tau_0/(R/2)$	Air, Carbopol	[D=0.23 m; PP(n_o=20, d_o=0.001m)], [D=0.76 m; RGS (D_S=0.35 m, H_S=1.95 m, n_o=128, d_o=0.0018-0.0023m)]
Mok et. al. (1990)	$\varepsilon = 0.107\times10^{-4}\,\mathrm{Re}_g^{1.09} Ga^{0.096}(d_o/D)^{-0.19}$	Oil free Air, Water, CMC (0.05, 0.075, 0.1, 0.15, 0.2, 0.3 wt%)	D=0.14 m PP (d_o=0.0003 m, n_o=51)
Ryu et. al. (1993)	$\varepsilon = 12.00 Fr^{1.220} Ga_{eff}^{0.025}$ in homogeneous flow $\varepsilon = 0.922 Fr^{-0.222} Ga_{eff}^{0.365}$ in churn-turbulent flow	Air, CMC (0.7 wt. %)	D=0.115 m RGS (D_S=0.038 m, H_S=0.15 m, d_o=5 μm)
Choi et. al. (1996)	$\varepsilon = 1.034 U_g^{0.704}$	Air, water, glass beads	0.456 m* 0.153m PP (d_o=0.002 m, n_o=30, 15)
Degaleesan et. al.	$\varepsilon = 0.07 U_g^{0.474-0.00626D}$, for D>0.1 m	Synthesis gas, Oil,	D = 0.46 m

(1997)		Mn particles	
Godbole et al. (1982)	$\varepsilon = 0.319 U_g^{0.476} \mu_l^{-0.058}$	Air, water, glycerine, CMC	D=0.305 m PP (d_o=0.00166 m, n_o=749)
Pohorecki et. al. (2001)	$\varepsilon_G = 0.383 U_g^{0.65} \sigma^{-0.52}$	N_2, Cyclohexane	D=0.304 m (d_o=0.001-0.005 m, n_o=1-27)
Jordan and Schumpe (2001)	$\frac{\varepsilon}{(1-\varepsilon)} = K_1 Bo^{0.16} Ga^{0.04} Fr^{0.70} \left[1 + 27.0 Fr^{0.52} \left(\frac{\rho_g}{\rho_l} \right)^{0.58} \right]$	N_2, He, Ethanol(96%),1-Butanol, Toluene, Decalin	D=0.1 m, PP (d_o=0.0043 m, n_o=1, d_o=0.001 m, n_o=1, d_o=0.001 m, n_o=19)
Syeda et. al. (2002)	$\varepsilon = 1.334 \left[(We/2)^{1/2} \right]^{0.032} \left(U_g \mu_l / \sigma \right)^{0.578} \left(\mu_l^4 g / \rho_l \sigma^3 \right)^{-0.131} \left(\rho_g / \rho_l \right)^{0.062} \left(\mu_g / \mu_l \right)^{0.107}$ In case of binary mixtures $(We_1/2)^{1/2}$ is replaced by $x(We_1/2)^{1/2} + (crk^2/\sigma) + (1-x)(We_2/2)^{1/2}$ Where $c = (2/CRT)\theta(x)(d\sigma/dx)$, $\theta(x) = x(1-x)/(1-x-xV_1/V_2)$ and $k = (12\pi\sigma/Ar)^{1/3}$; C=molar density of mixture	Air, water, methanol, 2-propanol, ethylene glycol	D=0.09 m PP (d_o=0.005 m, n_o=25, d_o=0.003 m, n_o=75)
Anabtawi et. al. (2003)	$\varepsilon = 0.362 U_g^{0.6} \mu_l^{-0.24} H^{-0.38}$; For cylindrical column $\varepsilon = 0.549 U_g^{0.81} \mu_l^{-0.15} H^{-0.22}$; For bi-directional column	Air, light oil, machine oil, engine oil	0.0195m * 0.22m, D = 0.074m, SN(d_o=0.01 m)
Urseanu et. al. (2003)	$\varepsilon = 0.21 U_g^{0.58} D^{-0.18} \mu_l^{-0.12} \rho_g^{\left[0.3\exp(-9\mu_l)\right]}$	N_2, tellus oil, glucose	[D = 0.15m, PP (d_o=0.0005 m, n_o=200)] [D = 0.23m, PP (d_o=0.0005 m, n_o=200), RGS (n_o=16, d_o=0.0015 m)]

Fransolet et. al. (2005)	$\varepsilon = 0.26 U_g^{0.54} \mu_{eff}^{-0.147}$	Air, water, xanthan	D = 0.24 m PP (d_o=0.001 m, n_o=203)
Mouza et. al. (2005)	$\varepsilon = 0.001\left[Fr'^{0.5}\, Ar^{0.1} Eo^{2.2} \left(d_s/D\right)\right]^{2/3}$	Air, water, butanol, glycerin	0.1 m * 0.1 m PoP (20, 40 μm)
Behkish et. al. (2006)	$\varepsilon = 0.00494\left(\rho_l^{0.415}\rho_g^{0.177}/\mu_l^{0.174}\sigma^{0.27}\right)U_g^{0.553}\left[P/(P-P_v)\right]^{0.203}\left[D/(D+1)\right]^{-0.117}$ $\left(K_d \times n_o d_o^{\alpha}\right)^{0.053} \exp\left[-2.231 C_S - 0.157\rho_P d_{32} - 0.242 X_W\right]$		Data available in literature is used for correlations
Kazakis et. al. (2007)	$\varepsilon = 0.2\left[Fr^{0.8} Ar^{0.2} Eo^{1.6} \left(d_s/D\right)^{0.9} \left(d_o/d_s\right)^{0.03}\right]^{2/5}$	Air, water, n-butanol, glycerin, kerosene	D = 0.09 m PoP (40, 100 μm)
Thaker and Rao (2007)	$\varepsilon = 1.4 U_g^{0.83} \left(H/D\right)^{0.09}$	Pure CO_2, distilled water, Aqueous NaOH solution (1N)	D=0.14 m PP (d_o=0.001 m, n_o=24)
Jin et. al. (2007)	$\varepsilon = 1.042 U_g^{0.523} \left(H/D\right)^{-0.096}$	Air, water	D = 0.16 m PP (d_o=0.001 m, n_o=55)
Anastasiou et. al. (2010)	$\varepsilon = 0.14\left[Fr^{1.0} Ar^{0.15} Eo^{1.85} \left(d_s/D\right)^{0.2} \left(d_o/d_s\right)^{-0.3}\right]^{0.37}$; For ionic surfactants $\varepsilon = 0.0034\left[Fr^{0.6} Ar^{0.15} Eo^{1.85} \left(d_s/D\right)^{0.2} \left(d_o/d_s\right)^{-0.3}\right]^{0.52}$ For non-ionic surfactans	Air, TritonX-100, SDS, CTAB	D = 0.09 m PoP (40 μm)
Maceiras et. al. (2010)	$\varepsilon = 1.83\times10^{-9} Fr^{0.45} Ar^{0.62} Eo^{0.7} \left(d_{32}/D\right)^{-1.3}$	CO_2, diethanolamine	0.06x0.06m column; PoP (d_o=0.004 m)
Asgharpour et. al. (2010)	$\varepsilon = 0.55 d_{32}^{0.101} U_g^{0.925} \sigma^{-0.54}$	Air, Distilled water (n-decane, n-tridecane, n-hexadecane used as	D=0.095 m PP (d_o=0.0003 m, n_o=26)

		impurities)	
Cachaza et. al. (2011)	$\varepsilon = 1.83U_g^{0.97}\left(C/C_t\right)^{0.08}$; C=conc. of surfactant, C_t=conc. of surfactant at flow transition. In absence of surfactant C/C_t=1	Air, water, $CaCl_2$, NaCl, KCl, EtOH, POH, IBOH	0.2 m * 0.04 m PP (d_o=0.001 m)
Anastasiou et. al. (2013)	$\varepsilon = 2.2\left[Fr^{1.07} Ar^{0.84} Eo^{0.19} \left(d_o/D\right)^{1.16} \left(d_o/d_s\right)^{2.86} \right]^{0.264}$	Air, glycerin, xanthan	D = 0.09 m PoP (40 μm)
Jin et. al. (2013)	$\varepsilon = 0.2064U_g^{0.787}\left(n_o d_o^2/D^2\right)^{-0.674} d_o^{-0.178}\left(\theta\pi/180\right)^{-0.203}$	Air, water	D = 0.3 m PP(d_o=0.002 m, n_o=98)
Sal et. al. (2013)	$\varepsilon_G = 0.2278\left(Fr^{0.7767} Ar^{0.3649}\left(d_o/D\right)^{0.4780}\right)\Big/\left(Eo^{0.3916} We^{0.2402}\right)$	Air, water	D = 0.33 m PP(d_o=0.001 m, n_o=817; d_o=0.002 m, n_o=217; d_o=0.003 m, n_o=91)
Kojima et. al. (1997)	$\varepsilon = 1.18U_g^{0.679}(\sigma/0.076)^{-0.546} \times \exp[K_1(\rho_l Q^2 d_o^{-3}\sigma^{-1})(P/P_o)^{K_2}]$ The constants K_1 and K_2 depends upon enzyme conc. Q =volumetric flow rate of gas	N_2 - O_2, water, NaH_2PO_4-citric acid solution, glucose oxidase	D = 0.045 m SN(d_o=0.00138, 0.0021, 0.0029, 0.00403 m)

Anabtawi et. al. (2003) studied effect of column geometry on gas hold up in cylindrical and bi-dimensional bubble columns using single nozzle sparger. Due to different dependence upon superficial gas velocity, static bed height and viscosity, separate corraltions were proposed for the two columns. The gas holdup decreased with increasing static bed height.

2.3 Bubble Diameter

A vast literature on Bubble diameter in bubble column is available. Some of the correlations are presented in Table 2.2. Different techniques were used to measure bubble diameter in a bubble column. Akita and Yoshida (1974), Jamialahmadi et al. (2001), Pohorecki et al. (2001, 2005) and Kanaris et al. (2018) used photographic technique for study. Researchers carried out experiments with different types of spargers like single nozzle, perforated plate, porous plate, etc. Akita and Yoshida (1974) and Kumar et al. (1976) carried out experiments in bubble column with different nozzle diameter and gas-liquid systems. Akita and Yoshida (1974) proposed a correlation in terms of dimensionless numbers, *Bo*, *Ga* and *Fr*. However; they did not include the influence of nozzle diameter in their correlation. It was observed that Sauter mean bubble diameter, d_{32}, decreases with increasing column diameter. Kumar et al. (1976) included nozzle diameter, d_o, in the correlation and proposed three different correlations for different range of *Re*. Gaddis and Vogelpohl (1986) combined flow rate as one of the parameters in addition to d_o. Gas velocity through a nozzle was used as parameter. Hinze (1955) developed an equation based on turbulence to estimate maximum diameter of bubble.

Jamialahmadi et al. (2001) propsoed a correlation for ratio of bubble diameter, d_b to d_o. The value d_b increases with liquid vicosity at high gas flow rate and remains constant with static bed height. Mok et al. (1990) found d_b to increase with increasing superficial gas velocity.

Kanaris et. al. (2018) and Feng et. al. (2019) proposed correlation for d_{32}/D as a function of *We*, *Re*, *Fr* and d_o/D. Value of d_{32} increases axially i.e., from bottom to top of the column. Jamshidi and Mostoufi (2017) proposed a correlation for ratio of maximum bubble chord length to column diameter. Aziz et. al. (2019) proposed correlations for initial bubble size and mean bubble size in terms of *Re*, *Eo* and sparger geometry parameter, n_o and pore diamter δ. The dimensionless numbers were estimated for gas velocity at the nozzle

In literature contrary results have been reported. Pohorecki et al. (1999) observed that value of d_{32} is constant. Later Pohorecki et al. (2001) observed that d_{32} decreases with increasing U_g and proposed a correlation only in terms of U_g. Similar result has been reported by Akita and Yoshida (1974). Later Pohorecki et al. (2005) included influence of fluid properties and U_g in their correlation. Apart from other researchers, correlation of Walter and Blanch (1983) shows the influence of both liquid and gas phase properties.

A close review of the correlations presented in Table 2.2 and from the discussion, it is clear that sparger parameters seem to be an important parameter for estimation of bubble diameter. The relationship between the two may also depend upon the flow regime. Another point is that while some of the investigator used volume average diameter of the bubble, d_b, other used d_{32}. The latter is more useful as specific interfacial area can easily be evaluated in terms of d_{32}.

Table 2.2: Correlations for bubble diameter, d_{32} in bubble columns

Investigator	Correlation	System	Column	Conditions	Remarks
Akita and Yoshida (1974)	$d_{32}/D = 26Bo^{-0.5}Ga^{-0.12}Fr^{-0.12}$	Air, water, glycol (30,70,100%), glycerol (25,45,65%), methanol, Sodium sulphite solution (0.15M)	Square Cross Section (0.15 m^2) PP[(d_o=0.0004 m, n_o = 52,105,247), [(d_o=0.0006 m, n_o = 52,105,247), [(d_o=0.0008 m, n_o = 52,105,247), [(d_o=0.001 m, n_o = 27,52,105,247), [(d_o=0.002 m, n_o = 247) PoP(0.00012-0.0001, 0.00005-0.00005, 0.00003-0.00002, 0.00001-0.000005 m) Square Cross Section [D=0.077 m^2 (SN d_o=0.003 m), D=0.15 m^2 (SN d_o=0.001, 0.002, 0.0045 m), D=0.2 m^2 (SN d_o=0.005 m)]	$U_g \leq$ 0.417 m/s, $\varepsilon_g \leq$ 30%	d_{32} dec. with inc. in D
Kumar et. al. (1976)	For $1 < Re < 10$ $d_{32} = 1.56(\mathrm{Re})^{0.058}\left(\sigma d_o^2/\Delta\rho_l g\right)^{1/4}$ For $10 < Re < 2100$ $d_{32} = 0.32(\mathrm{Re})^{0.425}\left(\sigma d_o^2/\Delta\rho_l g\right)^{1/4}$ For $4000 < Re < 70000$ $d_{32} = 100(\mathrm{Re})^{0.4}\left(\sigma d_o^2/\Delta\rho_l g\right)^{1/4}$	Air, Water, Glycerol (40%),, Kerosene CO_2, Aqueous NaOH (2M)	D=0.05, 0.075, 0.1 m SN (d_o=0.00087, 0.00153, 0.00196, 0.00265, 0.00309 m, n_o=1)	$U_g \leq 0.14$ m/s	

Gaddis and Vogelpohl (1986)	$d_b = \left[\left(\frac{6 d_o \sigma}{\rho_l g} \right)^{4/3} + \left(\frac{81 \mu_l Q_o}{\pi g \rho_l} \right) + \left(\frac{135 Q_o^2}{4 \pi^2 g} \right)^{4/5} \right]^{1/4}$	Air, Water, Glycerol	SN (d_o=0.0002-0.006 m, n_o=1)	$Q_o \leq 35*10^{-6}$ m^3/s	
Hinze (1955)	$d_b = 0.725 (\sigma/\rho_l)^{0.6} (U_o g)^{-0.4}$				
Walter and Blanch (1983)	$d_b = (\sigma/\rho_l)^{0.6} (\mu_l/\mu_g)^{0.1} (U_o g)^{-0.4}$				
Pohorecki et. al. (2005)	$d_{32} = 0.289 \rho_l^{-0.552} \mu_l^{-0.048} \sigma^{0.442} U_g^{-0.124}$	Air, Acetaldehyde, Acetone, Cyclohexane, Isopropanol, Methanol, N-Heptane, Toluene N_2, Cyclohexane, Water	D=0.09, 0.304 m PP (d_o=0.001-0.005 m, n_o=1-27)	$U_g \leq 0.05$ m/s	
Jamialahmadi et. al. (2001)	$d_b/d_o = \left[\left(\frac{5.0}{Bo_b^{1.08}} \right) + 9.261 \left(\frac{Fr^{0.36}}{Ga^{0.39}} \right) + 2.147 Fr^{0.51} \right]^{1/3}$	Air, Water, methanol, ethanol, propanol, isopropanol, glycerol, KCl	D = 0.05 m, H = 1.5 m	$Q_o \leq 0.15 *10^{-4}$ m^3/s	At high Q_o, d_b inc with μ_l
Mok et. al. (1990)	$d_b (\rho_l g / d_o \sigma)^{1/3} = 2.61 (We / Fr^{0.5})^{0.182}$	Oil free Air, Water, CMC (0.05, 0.075, 0.1, 0.15, 0.2, 0.3 wt%)	D=0.14 m PP (d_o=0.0003 m, n_o=51)	$U_g \leq$ 0.0504 m/s,	d_b inc. with U_g, d_b is larger at 0.3% CMC
Pohorecki et al. (2001)	$d_{32} = 1.658 \times 10^{-3} U_g^{-0.12}$	N_2, Cyclohexane	D=0.304 m PP (d_o=0.001-0.005 m, n_o=1-27)	$0.002 \leq U_g \leq 0.055$ m/s, $U_l \leq 1.4$ *	d_{32} dec. with U_g

				10^{-3} m/s,	
Jamshidi and Mostoufi (2018)	$\frac{d_b^{'}}{D} = 3.85*10^{2} Fr^{0.7} Ga^{-0.2} Bo^{-0.3}$	Air, water, CMC	D = 0.09 m, H = 1.75 m, PP(no = 100, do = 0.0005 m)	$0.5 \leq U_g \leq 7$ m/s, $0.00139 \leq \mu \leq 0.089$ Pa.s	
Kanaris et. al. (2018)	$\frac{d_{32}}{D} = 0.9\left[We^{0.95}\,\mathrm{Re}^{0.40}\,Fr^{0.47}\left(\frac{d_o}{D}\right)^{0.55}\right]^{0.51}$	Air, CO_2, He, water, glycerin	PoP(0.00004 m, 0.0001m)	$U_g \leq 0.2$ m/s, $\varepsilon_g \leq$ 8.4%	
Mouza (2018)	$\frac{d_{32}}{d_s} = 12.5\left[We^{-15.87}\,\mathrm{Re}^{13.73}\,Fr^{9.19}\left(\frac{d_o}{d_s}\right)^{2.77}\right]$	Air, water, glycerine, butanol, xanthan gum	PoP(0.00004 m, 0.0001 m)	$U_g \leq 3.35$ m/s	
Azizi et. al. (2019)	$d_i = 2.19*10^{-9} d_o\,\mathrm{Re}_{d_o}^{1.46} Eo_{d_o}^{-0.52}$ $d_m = 6.75*10^{-6}\frac{\sigma^2}{g\mu_l^2}\left(\frac{D}{n_o\delta_p}\right)^{0.47}\mathrm{Re}_{d_i}^{0.34}$	Air, water	D = 0.1 m, H = 1 m, Needles(n_o = 13, 19, 31, 42, 73, 115), (δ_p = 0.027, 0.021, 0.016, 0.014, 0.009, 0.008 m)	H_s = 0.7 m, $U_g \leq 0.095$ m/s	d_m inc. with Re and n_o, and dec. with δ_p
Feng et. al. (2019)	$\frac{d_{32}}{D} = 0.35\left[We^{0.95}\,\mathrm{Re}^{0.40}\,Fr^{0.47}\left(\frac{d_o}{D}\right)^{0.55}\right]^{0.09}$	N_2, He, water, ethanol	D = 0.01 m, H = 0.1 m SN (d_o=0.00008, n_o=1)	$U_g \leq 0.00276$ m/s $U_l \leq 0.00122$ m/s	d_{32} inc with U_g, d_{32} inc axially from bottom to top

2.4 Bubble aspect ratio

A vast literature on the study of bubble aspect ratio in two phase bubble column is available. Various shapes of the bubbles have been reported in literature. Clift et al. (1978) mentioned spherical, wobbling, ellipsoidal, spherical cap, skirted and dimpled-spherical cap bubbles. A shape region diagram showing the effect of Reynolds number, Eotvos number and Morton number on the shape of the bubbles was prepared. Very small bubbles (equivalent diameter < 1mm for air-water system) were considered as spherical bubbles. Since bubbles are never truly spherical, those having minor axis to major axis ratio within 10% of unity (i.e. 0.9 to 1.0) were considered spherical bubbles [Clift et al. (1978)]. Ellipsoidal bubbles were observed up to equivalent diameter < 20 mm. For equivalent diameter > 20 mm, spherical cap bubbles were observed. In bubble columns, sparger-hole diameter is generally much smaller than 20 mm. Hence, in most of the cases, at low gas velocity, ellipsoidal bubbles may be expected. It is applicable to range of parameters studied in the present work.

The bubble shape is expressed in terms of the aspect ratio, defined as ratio of minor axis to major axis. For defining the shape of bubbles as 'spherical cap' or 'ellipsoidal cap' bubbles, height of bubble, h, and breadth of bubble, b, are also used to define the aspect ratio (Fig. 2.2).

Few correlations for bubble shape are presented in Table 2.3. Correlations were proposed in terms of Weber number, *We*, *Mo*, *Re* and Tadaki number, *Ta*. Different techniques were used for study of bubble aspect ratio in bubble column. Among these, Raymond and Rosant (2000) used photographic technique for study bubble shape. Raymond and Rosant (2000) and Legendre et. al. (2012) covered a wide range of *Mo*. Bubble deformation decreases with *Mo*. Zhen et. al. (2019) found that with increase of pressure, aspect ratio increases, *E*, whereas, with increase of temperature influence of pressure on aspect ratio decreases.

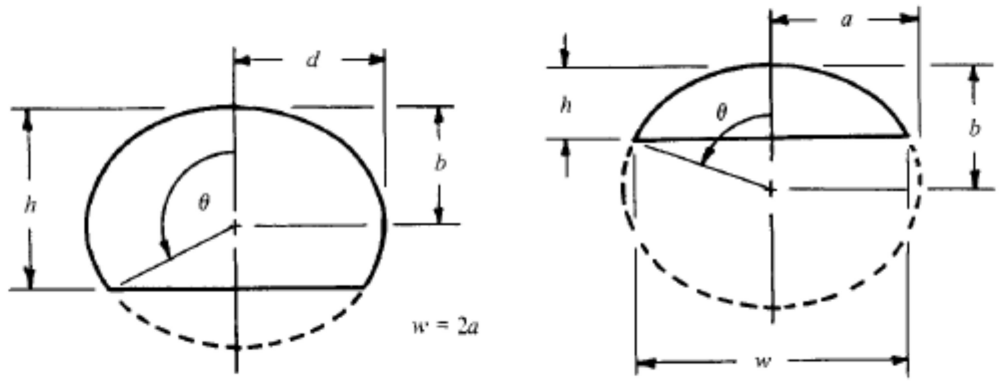

Figure 2.2: Parameters defining bubble shape for ellipsoidal bubbles (a) $\theta>90^{o}$ (b) $\theta<90^{o}$

[Bhaga and Weber (1981)]

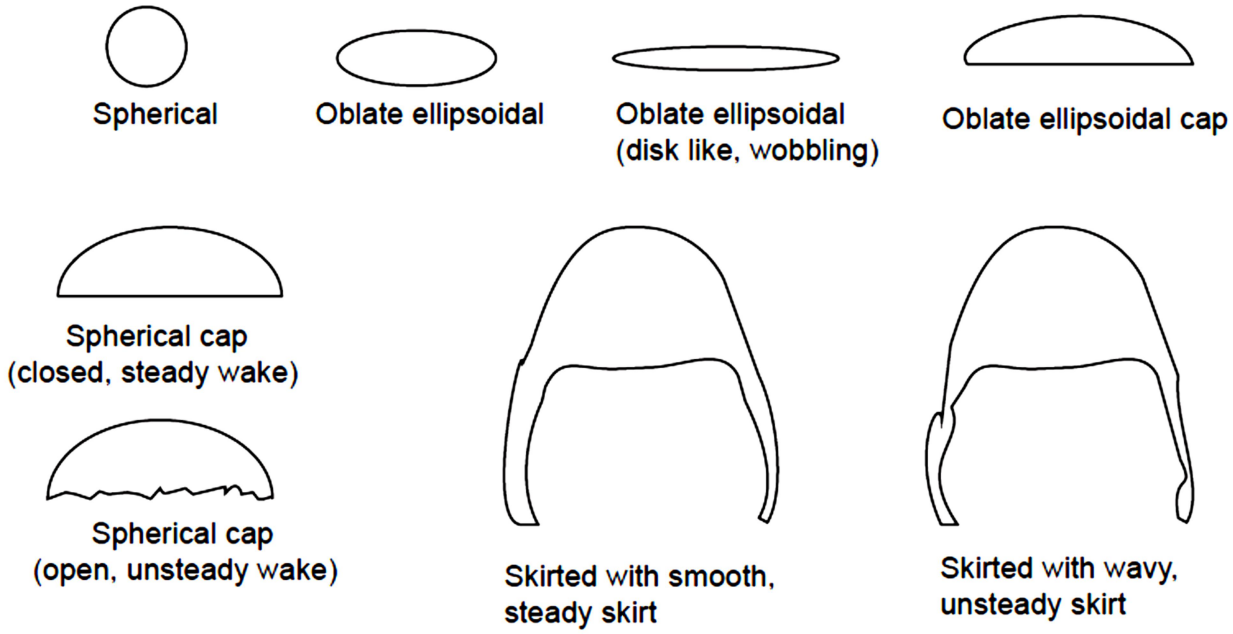

Figure 2.3 Different bubble shapes [Fan and Tsuchiya (1990)]

Since the drag force acting on the bubble depends upon the projected area of the bubble, which changes with aspect ratio, the consideration of the bubble shape is important. Fan and Tsuchiya (1990) gave a detailed description of bubble shapes as shown in Figure 2.3. The correlation given by Fan and Tsuchiya (1990) predicted spherical bubbles for $Ta < 1$ and spherical-cap bubbles for $Ta > 39.8$. The bubbles for other values of Ta were oblate ellipsoidal.

There are other types of bubble shape such as spherical cap bubbles with skirt, which were not observed in the present work. The formation of these bubbles depends upon the nature of the wake behind the bubble, which itself depend upon the Reynolds number. As the Reynolds number increase, closed wake behind bubble appears, increases in size and then converts into open wake. This phenomena deforms the bubbles from spherical to ellipsoidal and then to spherical cap and finally to skirted. There may be pimples at the bubble surface which may be due to local hydrodynamic environment of scale smaller than the size of the bubble.

Thus, it is expected that for air-eater system at moderate gas velocity in a small bubble column will be spherical, ellipsoidal or bubble cap. All these shapes are never perfect. A small deformation in the shape of bubble is always probable. However, if all the bubbles are considered as ellipsoidal, estimation of d_{32}, bubble volume, surface area can easily be made.

2.5 Specific Interfacial Area

Specific interfacial area in bubble columns has been reported by several investigators. It is easily estimated from the value of d_{32}. Interfacial area has been defined in literature in two ways. Earlier investigators estimated specific interfacial area as surface area per unit volume of gas-liquid dispersion [Pohorecki et al. (1999), Buchholz et al. (1979), Ryu et al. (1993)].

Table 2.3: Correlations for aspect ratio in bubble columns [Tadaki number, $Ta = g^{1/4} d_b U_{bs} \left(\rho_L/\sigma\right)^{3/4}$]

Investigator	Correlation	System	Column	Conditions	Remarks
Moore (1959)	$We = 4E^{4/3} \frac{E^{-3} + E^{-1} - 2}{\left(E^{-2} - 1\right)^3} \left[E^{-2} \sec^{-1} E^{-1} - \left(E^{-2} - 1\right)^{1/2}\right]^2$			Mo < 3, E > 0.5	
Tadaki (1961)	$E^{1/3} = \begin{cases} 0.62 & 16.5 \le Ta \\ 1.36 Ta^{-0.28} & 6 \le Ta \le 16.5 \\ 1.14 Ta^{-0.176} & 2 \le Ta \le 6 \\ 1 & Ta \le 2 \end{cases}$				
Loth (2008)	$E = 1 - \left(1 - E_{\min}\right) \tanh\left[c_E We\right]$ where $E_{\min} = 0.25 + 0.55 \exp\left[-0.99 \,\mathrm{Re}\right] c_E$ $= 0.165 + 0.55 \exp\left[-0.3 \,\mathrm{Re}\right]$			0.2 < Re < 5000	
Raymond and Rosant (2000)	$E = 1 - \frac{We}{9}$ $We = f\left(Mo\right) \mathrm{Re}^{5/3}$ $f\left(Mo\right) = 0.42 Mo^{0.35}$	Air, water, glycerin	D = 0.009 m, H = 0.06 m	$9*10^{-7} \le$ Mo ≤ 7	
Legendre et. al. (2012)	$E = 1 - \frac{9}{64} We \left(1 + \left(0.2 Mo^{1/10}\right) We\right)^{-1}$	Air, water, glycerin	D = 0.09 m	$1.6*10^{-6} \le$ Mo $\le$ 1.24	Bubble deformation dec. with Mo
Fan and Tsuchiya (2013)	$E = \begin{cases} 1 & \le Ta \le 0.3 \\ 0.77 + 0.24 \tanh[1.9(0.4 - \log_{10} Ta)] & 0.3 \le Ta \le 20 \\ 0.3 & 20 \le Ta \end{cases}$				

Tian et. al. (2019)	$E = 0.51 + 0.14\log Mo + 0.055\log^2 Mo$ $We > 12$ $E = \frac{1}{\left(1 + 4.1\mathrm{Re}^{2.4}\right)^{0.056}}$ $We < 12; Mo > 3$ $E = \frac{1}{\left(1 + 0.056 Eo^{0.65}\,\mathrm{Re}^{0.94}\right)^{0.38}}$ $We < 12; Mo < 3$	N_2, silicone oil, paraffin	D = 0.05m, H = 0.6 m, SN	P = 0.1, 6 MPa, T=293-473 K	E increases. with increasing P, As T increases, effect of P on E decreases
Besagni and Inzoli (2019)	$E = \frac{1}{1 + 0.489 Eo^{0.148}}$ For air-water, batch mode $E = \frac{1}{1 + 0.777 Eo^{0.167}}$ For air-water, countercurrent $E = \frac{1}{1 + 0.489 Eo^{0.186}}$ For air-water-ethanol	Water, ethanol	D=0.24 m, H=3.0 m, Spider sparger with 6 arm and 28 holes	$0.0037 \le U_g \le 0.0188$ ms^{-1}	

$$a_i = 6\varepsilon / d_{32} \tag{2.1}$$

Recently specific interfacial area is being estimated as surface area per unit volume of liquid [Bouaifi et al. (2001), Díaz et al. (2009), Maceiras et al. (2010)].

$$a_i = 6\varepsilon / d_{32}(1-\varepsilon) \tag{2.2}$$

Correlations for interfacial area and operating conditions are presented in Table 2.4. Most of the correlations show no effect of viscosity of the liquid. Correlation by Schumpe and Deckwer (1982) predicts decrease of a_i with increasing viscosity. However, the correlation is only for slug flow regime, Akita and Yoshida (1973) carried out experiments in a column of square cross section with perforated plate and porous plate spargers. The correlation involved *Bo* and *Ga*. The values of a_i depend upon column diameter, *D* and gas holdup. Sada et al (1984) measured values of a_i in case of molten salts and fitted the data with the correlation proposed by Akita and Yoshida (1973).

Chen et al. (2008) performed experiments in a multi-stage bubble columns. Water and dilute solution of CMC were used as liquid. Interfacial area was found to be a function of superficial gas and liquid velocities.

Pohorecki et al. (1999) compared several correlations to predict the values of a_i and found that a_i increases with increasing U_g. Vazquez et. al. (2000) correlated their data in terms of *Re*, *Fr*, *Bo*, *Sc* and d_o/D was also included in the correlation. The *Fr* in their correlation was square of the *Fr* used by most of the investigator. Bouaifi et al (2001) proposed a_i to be proportional to power dissipated in a bubble column, $P_g/V_L = \rho_L g U_g$.

Table 2.4: Correlations for specific interfacial area, a_i in bubble columns. The dimensionless numbers used are Eotvos number or Bond's Number, $Eo = Bo = gD^2\rho_l/\sigma_l$; Morton number, $Mo = \mu_l^4 g/\rho_l\sigma^3$; Reynold's number, $\mathrm{Re} = DU_g\rho_l/\mu_l$; Froude number, $Fr = U_g/\sqrt{gD}$; ; Galileo Number, $Ga = gD^3\rho_l^2/\mu_l^2$

Investigator	Correlation	System	Column
Akita and Yoshida (1974)	$a_i D = (1/3)\, Bo^{0.5} Ga^{0.1} \varepsilon^{1.13}$	Air, water, glycol (30,70,100%), glycerol (25,45,65%), methanol, Sodium sulphite solution (0.15M)	Square Cross Section (0.15 m^2) PP[(d_o=0.0004 m, n_o = 52, 105,247), [(d_o=0.0006 m, n_o = 52,105,247), [(d_o=0.0008 m, n_o = 52,105,247), [(d_o=0.001 m, n_o = 27, 52, 105, 247),[(d_o=0.002 m, n_o = 247) PoP(0.00012-0.0001, 0.00005-0.00005, 0.00003-0.00002, 0.00001-0.000005 m) Square Cross Section [D=0.077 m^2 (SN d_o=0.003 m), D=0.15 m^2 (SN d_o=0.001, 0.002, 0.0045 m), D=0.2 m^2 (SN d_o=0.005 m)]
Kumar et. al. (1976)	For $100 < Re_o < 2100$ $a_i \,\mathrm{Re}_o^{0.425}\left(\frac{\sigma d_o^4}{\Delta\rho_l g}\right)^{1.4} = 13.650U_g^* - 9.094U_g^{*2} + 1.828U_g^{*3}$ For $4000 < Re_o < 70000$ $a_i \,\mathrm{Re}_o^{-0.4}\left(\frac{\sigma d_o^4}{\Delta\rho_l g}\right)^{1/4} = 0.0437U_g^* - 0.091U_g^{*2} + 0.0059U_g^{*3}$	Air, Water, Glycerol (40%),, Kerosene CO_2, Aqueous NaOH (2M)	D=0.05, 0.075, 0.1 m SN (d_o=0.00087, 0.00153, 0.00196, 0.00265, 0.00309 m, n_o=1)
Schumpe and	$a_i = 4.65\times10^{-2} U_G^{-0.51} \mu_{eff}^{-0.51}$; for slug flow only	Air,	D=0.102, 0.14 m

Deckwer (1982)		CMC (0-2%) Na_2SO_4 (0.8mol/l)	SP (d_o=0.00015, 0.0002 m) PP [(d_o=0.0005 m, n_o=421), (d_o=0.001 m, n_o=73), d_o=0.002 m, d_o=19)]
Chen et. al. (2008)	$a_i = 9271 U_G^{1.09}$	N_2-CO_2 mixture, water, $BaCl_2$, NaOH, $BaCO_3$	D=0.05 m PP (d_o=0.001 m, n_o=4/square cm)
Zhao et. al. (2004)	$a_i = 1480\sigma^{-0.00130} U_G^{0.634} e^{292/T}$	CO_2, Na_2CO_3-$NaHCO_3$ (0.5 mol/L) $NaAsO_2$ (0-0.008 mol/L, catalyst), DBS (0-5 mg/L, surface tension modifier)	D=0.102 m
Pohorecki et al. (1999)	$a_i = 1120 U_g^{0.63}$	N_2, water	D = 0.3 m, PP(d_o=0.001 m - 0.005 m, n_o= 1 - 27)
Bouaifi et al. (2001)	$a_i = 0.26\left(P_G / V_L\right)^{0.63} = 0.26\left(\rho_L g U_G\right)^{0.63}$	Air, water	D = 0.43 m, RGS (D_S=0.165 m, d_o=0.001 m, n_o= 90)
Vazquez et. al. (2000)	$a_i = 0.0046\,\mathrm{Re}^{0.98} Fr^{0.19} Bo^{-0.70} Sc^{0.57} \left(d_o / D\right)^{-0.19}$	Pure CO_2, Water, Buffer solution Na_2CO_3-$NaHCO_3$, Sodium Arsenite (Catalyst), SLS	D_i=0.113, D_o=0.148 m PoP (150-200, 90-150, 40-90 μm)
Besagni and Inzoli (2017)	$a_i = \left(0.23 / D\right) AR^{-0.3} Eo^{1/2} Ga^{0.12} Fr^{1/2}$	Deionized water, Aq. Soln of NaCl, Etanol and MEG	D=0.24; $5 \le AR(=H_o/D) \le 12.5$;

From Equation 2.1 it is clear that specific interfacial area is directly proportional to ε and inversely proportional to d_{32}. Due to change in the flow regime, it is difficult to get a single correlation for ε. It is also easy to understand that due to presence of bubble coalescence in churn-turbulent regime and its absence in homogenously bubbling regime, it is difficult to obtain a single correlation for d_{32}. Therefore, it is not proper to expect a single correlation for a_i. However, attempts were made to include ε in the correlation for a_i [Akita and Yoshida (1974), Besagni and Inzoli (2017)]. Few correlation for a_i taking only U_g as a parameter were also proposed [Pohorecki et al. (1999), Chen et. al. (2008)]. However, such correlation may fit a specific set of experimental data obtained for bubble columns operatd in a single flow regime. In the slug flow regime bubble interface is very close to the column wall and hence viscosity of fluid is expected to play crucial role in bubble behaviour. Correlation by Schumpe and Deckwer (1982) is applicable to slug flow regime only and includes U_g and effective viscosity. In general, a_i increases with increasing U_g. The value of a_i decreases with increasing viscosity [Schumpe and Deckwer (1982), Vazquez et. al. (2000)]. The value of a_i decreases with increasing temperature [Zhao et. al. (2004)].

2.6 Gas-Liquid Mass-transfer Coefficient ($k_L a_i$)

Volumetric mass-transfer coefficient in bubbles columns have been studied by several investigators. The effect of fluid properties, column diameter and type of sparger has been investigated and correlations have been proposed. Some of the correlations are presented in Table 2.5. Some of these correlations are for ($k_L a_i$) while other correlations are in terms of Sherwood number, Sh. A wide range of correlations are due to combination of k_L and a_i.

Table 2.5: Correlations for volumetric mass-transfer coefficient, $k_L a_i$ in bubble columns (PP=Perforated plate, SN=Single nozzle, SP=Sintered plate), PoP= Porous Plate, RGS= Radial Gas Sparger)

Investigator	Correlation	System	Column	Conditions	Remarks
Akita and Yoshida (1973)	$k_L a_i D^2 / D_L = 0.6 Sc^{0.5} Bo^{0.62} Ga^{0.21} \varepsilon^{1.1}$	Air, oxygen, helium/water, glycol, glycerol, methanol, 0.15M Sodium sulphite solution	D=0.152, 0.301, 0.6 m d_o=0.005 m, n_o = 1		
Akita and Yoshida (1974)	$Sh = \left(k_L d_{vs} / D_L\right) = 0.5 Sc^{1/2} Bo^{3/8} Ga^{1/4} \varepsilon^{1.1}$	Air, water, glycol (30,70,100%), glycerol (25,45,65%), methanol, Sodium sulphite solution (0.15M)	Square Cross Section (0.15 m^2) PP(d_o=0.0004 - 0.002 m, n_o = 27 – 247) PoP(0.00012-0.0001, 0.00005-0.00005, 0.00003-0.00002, 0.00001-0.000005 m) Square Cross Section [D=0.077 m^2 (SN d_o=0.003 m), D=0.15 m^2 (SN d_o=0.001, 0.002, 0.0045 m), D=0.2 m^2 (SN d_o=0.005 m)]	$U_g \leq$ 0.417 ms^{-1}, $\varepsilon_g \leq$ 30%	$k_L a_i$ inc. with inc. in D
Schumpe	$k_L = 0.0045 U_g^{0.08} \mu_{eff}^{-0.32}$	Air,	D=0.102, 0.14 m	$U_g \leq 0.2$ ms^{-1}	K_L varies

and Deckwer (1982)		CMC (0-2%) Na_2SO_4 (0.8mol/l)	SP (d_o=0.00015, 0.0002 m) PP (d_o=0.0005 – 0.002 m, n_o= 19 - 421)		very slightly with U_g
Sada et.a l. (1985)	$k_L = 0.014U_G^{-0.86}$ $k_G = 170U_G^{0.72}$	O_2/ NaCl, NaOH, $Ca(OH)_2$ 5% CO_2/ NaCl, NaOH, $Ca(OH)_2$	D=0.05 m PP (d_o=0.001 m, n_o=10)	$0.01 \le U_g \le 0.1$ ms^{-1}	
Sada et. al. (1986)	$k_L a = 0.24\varepsilon^{0.9}$	Ion-exchanged water, Sucrose, Na_2SO_4, NaCl, KCl, $Ca(OH)_2$, glass bead, nylon6, pure O_2, N_2	D=0.078 m PP (d_o=0.001 m, n_o=37)	$0.02 \le U_g \le 0.2$ ms^{-1}	
Ryu et. al. (1993)	For bubbly flow $k_L a_i D^2 / D_L = 4.95x10^7 Sc_{eff}^{-0.31} Fr^{0.16}$ For churn-turbulent flow $k_L a_i D^2 / D_L = 5.8x10^7 Sc_{eff}^{-0.345} Fr^{0.495}$	Air, CMC (0.7 wt. %)	D=0.115 m RGS ((D_S=0.038 m, H_S=0.15 m, d_o=5 μm	$0.009 \le U_g \le 0.098$ ms^{-1}	$k_L a_i$ dec. with inc. μ_l, type of sparger had a great impact on $k_L a_i$
Alvarez et. al. (2000)	$k_L a_i = K_1 U_g^{2/3} \sigma^{3/4} \mu_l^{-3/4} \rho_l^{3/2}$ $1.924x10^{-7}$, $1.969x10^{-7}$, $2.079x10^{-7}$ for different plates	Pure CO_2, Sucrose and Sodium Lauryl Sulphate Solution	D_i=0.113, D_o=0.148 m PoP (150-200, 90-150, 40-90 μm)		k_L dec. due to the presence of surfactants
Vazquez et. al. (2000a) Vazquez et. al. (2000b)	$k_L = K_1 \sigma^{1.35} U_g^{0.5}$; K_1 depends upon sparger	Pure CO_2, Water, Buffer solution Na_2CO_3-$NaHCO_3$, Sodium Arsenite (Catalyst), SLS	D_i=0.113, D_o=0.148 m PoP (150-200, 90-150, 40-90 μm)		

Jordan and Schumpe (2001)	$Sh = a_1 Sc^{0.5} Bo^{0.34} Ga^{0.37} Fr^{0.72} \left[1+13.2 Fr^{0.27} \left(\rho_g/\rho_l\right)^{0.49}\right]$ a_1= constant depending upon sparger	N_2, He, Ethanol(96%),1-Butanol, Toluene, Decalin	D=0.1 m, PP (d_o=0.0043 m, n_o=1, d_o=0.001 m, n_o=1, d_o=0.001 m, n_o=19	293≤ T≤343 K, $0.01 \le U_g \le 0.21$ ms^{-1},	k_L inc. with inc. in T
Behkish et. al. (2002)	$k_L a_i = 0.18 Sc^{0.6} \left(\rho_l v_A / M_B\right)^{-2.84} \times \left(\rho_g U_g\right)^{0.49} \exp\left(-2.66 C_{sv}\right)$ C_{SV}- volumetric solid conc.		Data available in literature is used for correlations	0.17≤ P ≤0.79 MPa, $0.05 \le U_g \le 0.25$ ms^{-1}	$k_L a_i$ inc. with inc. in P, U_g
Hughmark (1967)	$\left(k_L d_{32}/D_L\right) = 2 + 0.0187\,\mathrm{Re}^{0.779} Sc^{0.546} \times \left(d_{32} g^{1/3}/D_L^{2/3}\right)^{0.116}$	Air/water, Versol, Glycerol, Na_2CO_3 soln., $ZnCl_2$ soln.	D=0.0254, 0.0508, 0.1524, 0.3048m	$U_g \le 1$ foot.s^{-1}	
Baz-Rodriguez et. al. (2014)	$k_L/k_{Lw} = \left(1-\varepsilon\right)^{4.377} \times \left[2.12 Eo^{0.1906} - \exp\left(0.009016 c_r^2\right)\right]$	Air, NaCl (0.05, 0.13, 0.21, 0.29, 0.37 M), $CaCl_2$ (0.02, 0.04, 0.06, 0.08, 0.10 M), $MgCl_2$ (0.02, 0.04, 0.05, 0.08, 0.11, 0.14)	D=0.095 m, PoP (d_o= 160-250 μm)	$0.0005 \le U_g \le 0.0197$ ms^{-1}	k_L dec. due to the presence of electrolytes
Jin et. al. (2014)	$k_L a_i = 3.051 \times \left(\rho_l v_A / M_B\right)^{-1.193} \times Sc^{-0.734} \left(\rho_g U_g\right)^{0.524}$	H_2, CO, CO_2, paraffin, sand (particle size 150-200 μm)	D=0.1 m, PP (d_o=0.008 m, n_o=4)	293≤ T ≤473K, $1 \le P \le 3$ MPa, $0.03 \le U_g \le 0.1$ ms^{-1}	$k_L a_i$ inc. with inc. P, T, U_g
Zhao et. al. (2004)	$\ln(k_L) = 4.13 + 0.797 \ln(\sigma) + 0.411 \ln(U_g) - 2.59 \times 10^3/T$	CO_2, Na_2CO_3-$NaHCO_3$ (0.5 mol/L) $NaAsO_2$ (0-0.008 mol/L, catalyst), DBS (0-5 mg/L, surface tension modifier)	D=0.102 m	$0.013 \le U_g \le 0.031$ ms^{-1}	k_L inc. with inc. in U_g and T, presence of surfactant dec. k_L
Bhatia et. al. (2004)	$Sh = 2.0 + 0.6\,\mathrm{Re}^{0.5} Sc^{0.33}$	Air, Tap Water, alcohol ((0.5 volume %)	D=0.2 m, PP (d_o=0.0025 m, n_o=1256)	$0.05 \le U_g \le 0.0758$ ms^{-1}	Presence of alcohol inc. value of $k_L a_i$

Therning and Rasmuson (2006)	$k_L a_i = k_M D_L / D\, Sc^{0.5} Bo^{4/7} Ar^{2/7} \varepsilon^{1.18}$; k_M depends upon surface conc.	Air, deionized water,Na_2SO_3 (0.8 M), H_2SO_4 (0.06-0.035 M)	D=0.2 m, PP (d_o=0.002 m, n_o=69) D=0.05 m, PoP (d_o=5 μm, Plastic membrane)	$0.03 \leq U_g \leq 0.2$ ms^{-1}	$k_L a_i/\varepsilon$ is constant and equal to 0.5 for the systems used
Nedeltchev et. al. (2007)	$k_L a = f_c \sqrt{4 D_L R_{sf} / \pi S_B}\left(f_B S_B / A U_B\right)$ where $R_{sf} = \pi \sqrt{\left(l^2 + h^2\right)/2 - \left(l - h\right)/8.U_b}$ and $f_c = 0.124 Eo^{0.94}\left(\rho_G / 1.2\right)^{0.15}$			$0.1 \leq P \leq 4$ MPa	
Schaaf et. al. (2007)	$k_L a_i / \varepsilon = 3.0\sqrt{D U_b / d_b^3}$	Air, N_2, Demineralized water, organic oil (Isopar M, Exxon-Mobil)	D=0.15 m PP(D = 0.1 m, d_o= 0.0005 m)	$0.1 \leq P \leq 1.3$ MPa	$k_L a_i$ inc. with inc. in ε
Thaker and Rao (2007)	$k_L a_i = 1.87 U_g^{0.56}\left(H_s / D\right)^{-1.68}$	Pure CO_2, distilled water, Aqueous NaOH solution (1N)	D=0.14 m PP (d_o=0.001 m, n_o=24)	$0.003 \leq U_g \leq 0.045$ ms^{-1}	$k_L a_i$ dec. with inc. in H_s
Gomez-Diaz et. al. (2009)	$Sh = 6.7\,\mathrm{Re}^{0.6}\, Sc^{0.5}$	CO_2, k-carrageenan distilled water solution	D=0.07 m	$Qg \leq 30 L.hr^{-1}$	$k_L a_i$ inc. with inc. in U_g and dec. with inc. of μ_l
Asgharpour et. al. (2010)	$Sh = 0.15\,\mathrm{Re}^{2/3}\, Sc^{1/2} Bo^{2/3}$	Air, Distilled water (n-decane, n-tridecane, n-hexadecane used as impurities)	D=0.095 m PP (d_o=0.0003 m, n_o=26)	$0.00118 \leq U_g \leq 0.0235$ ms^{-1}	$k_L a_i$ inc. with inc. in U_g and alkane conc.

Correlation proposed by Akita and Yoshida (1973) was in terms of dimensionless numbers Sc, *Bo* and *Ga*, which may be estimated using physical properties of the fluids and column diameter as the only geometric parameter. Hughmark (1967) and Akita and Yoshida (1974) studied effect of bubble size on volumetric mass transfer coefficient. Schumpe and Deckwer (1982) measured specific interfacial area and using it in the correlation for $k_L a_i$ proposed by Deckwer et al. (1982) obtained an expression for gas-liquid mass-transfer coefficient. It did not include any physical propery of the fluid except effective viscosity.

Different approached to propose a correlation to predict mass-transfer coefficient were also made. Alvarez et al. (2000) studied volumetric mass-transfer coefficient in bubble column and proposed a correlation with different constant for different sparger. Vazquez et al. (2000a, 2000b) also observed that constant in their correlation depends upon the type of the sparger. The only physical property of the system was surface tension of the liquid. Jordan and Schumpe (2001) proposed correlation for Sherwood number, *Sh*, and observed different constant for different spargers.

Ryu et. al. (1993) proposed two correlations for volumetric mass transfer coefficient depending upon the type of flow i.e. bubbly flow and churn-turbulent flow. They concluded that sparger type has great impact on $k_L a_i$. Sada et. al. (1986) proposed a correlation only in terms of gas holdup. Correlations proposed by Akita and Yoshida (1973, 1974), Therning and Rasmuson (2006) and Schaaf et al. (2007) included gas holdup as a parameter. In this way the effect of sparger was indirectly included in these correlations.

Correlation by Schaaf et al. (2007) predicts the effect of both bbble size and bubble rise velocity on volumetric mass transfer coefficient. Correlation by Thaker and Rao (2007) predicts

the effect of static bed height on volumetric mass transfer coefficient. It predicts $k_L a_i$ to decrease with increase in static bed height.

A few attempts have also been to apply mass trasnfer theories in bubble columns. Nedeltchev et al. (2007) proposed a correction factor to penetration theory to correlate data on mass-transfer coefficient in bubble columns operated at high pressure.

It is well known that volumetric mass-transfer coeffient can be estimated by knowing mass-trasnfer coefficient and specifc interfacial area. However, such attempts are either missing or did not catch attention. It may be interesting to study the effect of sparger on mass-transfer coefficient and specifc interfacial area separately and search for a more reliable correlation.

Based on the above discussion it is clear that volumetric mass-transfer coefficient depends on specific interfacial area, which strongly depends upon the nozzle diameter. For better correlation of specific interfacial area it is necessary to study dependence of bubble diameter on other variables. Bubble size measurement to obtain bubble-size distribution is essential to have a good estimate of specific interfacial area. Bubble size is also related to bubble velocity and hence induces turbulence, which may give an estimate of mass-transfer coefficient.

Selection of a suitable measuring device is an important aspect. A few of the desirable qualities are non-intrusive and non-invasive nature of the technique, fast response, cost effectiveness, ability to sense tiny bubbles etc. In the following section some of the techniques tried in bubble columns are presented.

2.7 Measurement Techniques for Bubble Behaviour

A number of techniques have been used to study hydrodynamics and other parameters related to bubble behaviour in bubble column. These techniques may be broadly classified as photographic, probe-technique, tomography, radiography, acoustic method etc. Earlier works used photographic technique to study bubble behaviour [Akita and Yoshida (1974), Ryu et al. (1993), Gomez-Diaz et al. (2009)]. Availability of image processing techniques made this technique a more powerful measuring technique. A brief literature is reviewed in the following section. A few of the work using photographic technique is presented in Table 2.6.

2.7.1 Photographic Technique

Photographic technique has been a popular technique as it directly obtains images or video which can be analysed later. It is a visualization technique, hence, seems more convincing than other techniques. Though, measurement of size and shape of the bubbles and bubble velocity by this method is considered as the direct method, it is a time consuming task if done manually. Recently investigations in bubble column have been carried using efficient image processing methods for measuring these parameters [Karn et al. (2015), Ahmed et al. (2015), Lau et al. (2013a, b), Fu and Liu (2016), Besagni and Inzoli (2016a, b)]. One of the challenges faced by image processing technique is identification of overlapping bubbles. Such a situation occurs when gas holdup is large. Improper illumination, video recording rate (frames per second), pixel size are other aspects of digital photographic technique which should be considered. It affects the choice of camera and image processing technique.

Table 2.6: Use of photographic technique to study bubble behaviour

Investigator	Test section or Column; Sparger	System	Measurements
Kojima et al. (1968)	0.2×0.2×0.3m; Single bubbles	Castor oil, Glycerine, Corn syrup	AR, U_{bs}; 10 Images per s
Camarasa et al. (1999)	ID=0.1 m, H=2 m, one nozzle (d_o=0.005m), 62 holes (d_o=0.001m)	Air/water, aq. Soln. of pentanol and butanol	Shutter speed (1/1200s, 1/4000s); BSD, d_{eq}
Majumder et al. (2006)	D= m; d_o=0.004, 0.005, 0.006 and 0.007 m;	Air/water	BSD, d_{32}, a_i; Images
Zaruba et. al.(2005)	0.1×0.02×1.5m	Air-water	U_b profile, BSD and dispersion coefficient; 500fps
Cordero et. al. (2012)	0.05×0.1m	N_2-Boger	Bubble size and U_b
Lau et. al. (2013b)	0.2×0.03×1m	Air-water	U_b, ε_g and BSD
Amirnia et. al. (2013)	0.27×0.3×2.4m	Air-CMC and xanthan gum	Terminal rise velocity of bubbles, bubble shape

Ahmed et. al. (2015)	0.432×0.013×1.815m	Water-gas	ε_g and U_b profiles
Besagni and Inzoli, (2016a,b)	0.24×5.3m	Air-water	ε_g , swarm velocity, BSD, AR, orientation of bubbles
Fu and Liu, 2016	0.203×0.344	Water-gas	BSD and distribution of area, perimeter, major axis, minor axis, roundness and eccentricity of bubbles
Sasaki et. al., 2016	0.2×2m	Air-water	ε_g
Besagni et. al., 2016b	0.24×5.3m	Air-water and ethanol solution	ε_g, flow regime transition, bubble shape and BSD

Zaruba et. al. (2005) studied hydrodynamics in a small rectangular bubble column by capturing images at 500 fps for superficial gas velocity ranging from 0.0005 to 0.004 $m.s^{-1}$. A bubble recognition algorithm was developed and used to tracking individual bubbles based on the bright spot at the centre of the bubble. Time-averaged velocity profiles and turbulent diffusion coefficients were derived as a function of the superficial gas velocity. Turbulent diffusion coefficient of the gaseous phase followed Gaussian standard distribution. An image processing algorithm generally involves both bubble segmentation and reconstruction techniques. Cordero et al. (2012) used image processing technique to study terminal rise velocity of single bubbles and swarm of bubbles in elastic fluids. Conditions for formation of bubble clusters and its dependence on the bubble size were studied. Free rise of small air bubbles in aqueous solutions of xanthan gum and carboxymethylcellulose was studied [Amirnia et al. (2013)].

Algorithms such as watershed algorithm [Lau, et al. (2013a, b)] and the algorithm combining geometrical, optical and topological information [Fu and Liu (2016)] were applied to process the high-speed bubbly flow images in gas-liquid contactors.

A robust image measurement technique was proposed to measure the bubble size distribution in dense bubbly flows with wide size range of 120 mm–4 mm and void fractions in the range of 0.02–0.7 [Karn et al. (2015)]. It classifies bubbles into different categories based on their morphology and size. Considering that there is an intensity gradient at the center of individual bubble, the bubble clusters are segmented into individual bubbles. The proposed technique was able to capture the size, shape and location information of all.

The shape of the bubbles and the path were studied with high speed camera using image processing software. A robust and accurate recursive algorithm was developed for concave point

extraction. It involved a reconstruction method based on a template database. However, it was illustrated for gas holdup < 0.056 [Zhong et al. (2013)]. The problem associated with measurement of shape of bubbles is that the bubbles in a bubble column are not perfect sphere. They are deformed while moving in the column. The common shapes of bubbles are nearly spherical, ellipsoidal and spherical cap bubbles. Large bubbles generally are of irregular shape. These bubbles are often described in terms of aspect ratio, which is a measure of deviation from perfect sphere.

Use of image analysis to study the effect of gas velocity, liquid velocity and sparger geometry on bubble-size distribution was illustrated in a counter-current bubble column of 0.24 m inner diameter and 5.3 m height with gas superficial velocities in the range of 0.004–0.20 $m.s^{-1}$ and liquid superficial velocities up to 0.09 $m.s^{-1}$. In the batch mode, the bubble size distribution was poly-dispersed and bimodal. The transition from homogeneous to turbulent flow, bubble vertical velocity and qualitative behaviour of local bubble size was also discussed [Besagni and Inzoli (2016a)]. Later the effect of superficial gas and liquid velocities on bubble-size distribution, aspect ratio and bubble orientation was studied in an annular gap bubble column for gas holdup in the range of 0.029 to 0.096 [Besagni and Inzoli (2016b)]. In this range homogeneous flow regime dominates. A correlation between for aspect ratio in terms of non-dimensional parameters was obtained. The image analysis was also used for the evaluation of the gas velocity at which the transition occurs. Effect of addition of ethanol on gas holdup, flow regime transition and bubble size distribution in a large-diameter and large-scale bubble column (0.24 m inner diameter and 5.3 m height) was studied [Bersagni et al. (2016)].

Sasaki et al. (2016) studied effect of static bed height on gas holdup and flow structure in rectangular and cylindrical bubble columns using image processing technique and an empirical correlation for gas holdup was proposed for superficial gas velocity in the range of 0.025 to 0.40 $m.s^{-1}$. Bubbles of various sizes were observed. Column-scale vortical structures induced by rising motion of bubble swarms were studied.

Ahmed et al. (2015) used conversion of high speed camera images into binary images followed by watershed segmentation to study the gas holdup in a rectangular bubble column. Variation of gas holdup in the horizontal directions was obtained. The results were comparable with that obtained by using a 4 point optical probe.

Thus, it can be concluded that using image processing technique of images obtained from high speed camera various dynamic features of the hydrodynamic parameters can be studied in bubble columns. Photographic technique is a direct method. The images are obtained either by an external camera facing a transparent column wall or by using optical probes [Ahmed et al. (2015)] placed at one or more locations in the column. The former is a non-invasive method and location, shape and size of all bubbles are captured simultaneously. Bubble velocity can also be estimated from sequence of images. Use of optical probes can be used in columns which do not have transparent walls. However, only local images are obtained. Estimation of hydrodynamic behaviour is not direct and not all bubble parameters can be measured. In the present work, image processing technique was used to study the effect of superficial gas velocity and static bed heights on gas holdup and dynamic nature of the expanded bed height.

2.8 Objective of the present work

The present work is aimed at measurement of bubble behaviour in a rectangular bubble column using photographic technique:-

(i) To develop image-processing algorithm for measurement of instantaneous expanded bed height, foam layer thickness and thickness entry region.

(ii) To develop image-processing algorithm to identify bubbles and to determine number of bubbles and parameter related to their size e.g. major and minor axis.

(iii) To determine bubble size distribution (BSD), gas holdup, Sauter mean diameter and specific interfacial area for Newtonian and power law fluids (aqueous solution of CMC).

(iv) To study the effect of superficial gas velocity and static bed height and fluid properties on BSD, gas holdup, Sauter mean bubble diameter and specific interfacial area.

(v) To develop a methodology for the prediction of mass-transfer coefficient.

The next chapter describes the details of the experimental set-up, experimental procedures, fluid properties, procedure for analysis of the image analysis data.